

Klug, Florian

Article — Published Version

Synchronization and stability in automotive transportation networks

Naval Research Logistics (NRL)

Provided in Cooperation with:

John Wiley & Sons

Suggested Citation: Klug, Florian (2022) : Synchronization and stability in automotive transportation networks, Naval Research Logistics (NRL), ISSN 1520-6750, John Wiley & Sons, Inc., Hoboken, USA, Vol. 70, Iss. 2, pp. 165-183, <https://doi.org/10.1002/nav.22089>

This Version is available at:

<https://hdl.handle.net/10419/287872>

Standard-Nutzungsbedingungen:

Die Dokumente auf EconStor dürfen zu eigenen wissenschaftlichen Zwecken und zum Privatgebrauch gespeichert und kopiert werden.

Sie dürfen die Dokumente nicht für öffentliche oder kommerzielle Zwecke vervielfältigen, öffentlich ausstellen, öffentlich zugänglich machen, vertreiben oder anderweitig nutzen.

Sofern die Verfasser die Dokumente unter Open-Content-Lizenzen (insbesondere CC-Lizenzen) zur Verfügung gestellt haben sollten, gelten abweichend von diesen Nutzungsbedingungen die in der dort genannten Lizenz gewährten Nutzungsrechte.

Terms of use:

Documents in EconStor may be saved and copied for your personal and scholarly purposes.

You are not to copy documents for public or commercial purposes, to exhibit the documents publicly, to make them publicly available on the internet, or to distribute or otherwise use the documents in public.

If the documents have been made available under an Open Content Licence (especially Creative Commons Licences), you may exercise further usage rights as specified in the indicated licence.



<http://creativecommons.org/licenses/by-nc/4.0/>

RESEARCH ARTICLE

Synchronization and stability in automotive transportation networks

Florian Klug 

Department of Business Administration, Munich University of Applied Sciences, München, Germany

Correspondence

Florian Klug, Department of Business Administration, Munich University of Applied Sciences, Am Stadtpark 20, D-81243 München, Germany.
Email: florian.klug@hm.edu

History

Accepted by Xin Chen, logistics and supply chain management.

Abstract

The aim of this study was to analyze and evaluate synchronization and stability issues for the planning, operation, and control of processes in automotive transportation networks. We modeled transportation networks by using a coupled oscillator network based on a modified Kuramoto model. Each transport process was mapped as a phase oscillator indicating the transport time, period, and delay. The method could be applied to complex networks where it has not been possible to find analytical solutions. The novel generic oscillator approach was then applied to two transport topologies, namely, milk-run and just-in-sequence transport, based on real-world problems from a German car manufacturer. We conducted a detailed study of the parameter regions where different synchronization regimes occurred and investigated how the topology influenced the stability and dynamic behavior of transport networks. In particular, we focused on how transport period offsets and transport delays affected synchronous states. We showed that by the introduction of a transport synchronization matrix, the synchronization states in a transport network could be represented in a compact and comprehensive manner. Moreover, thresholds for round-trip stability could be calculated by analyzing the phase decoupling of a milk-run. These results were used for the vehicle route planning of milk-runs with synchronization constraints. Furthermore, the influence of the time delay of a track and trace system on the transport synchronization was analyzed. Finally, for the subsequent investigation of a just-in-sequence transport network, we showed how an adaptive control mechanism could re-synchronize an out-of-tune delivery process.

KEYWORDS

just-in-sequence transport, network synchronization, track and trace system, transport planning, transportation networks, vehicle routing

1 | INTRODUCTION

Independent of the consideration of a specific means of transport or transport relation, there are general questions regarding the interactions among the resources involved. These are, among others, “How often and at what time a transport runs?,” “Are there any delays?,” and, if so, “What influence does the transport delay have on upstream and downstream

processes?” In order to create harmonized and thus efficient transport relations, it is important that transports are highly coordinated and orchestrated in terms of both quantity and time. Improper transport synchronization can lead to transitions and instabilities that cause very complex dynamics. The synchronization of upstream and downstream transport processes can lead to significant performance improvements through increased goods speed, inventory reduction,

improved responsiveness, and better long-term planning (Klug, 2017). By combining the fundamental questions of transport management with the dynamic rhythmic representation of oscillators, we can develop new methods to analyze synchronization and stability in transportation networks. The purpose of this study was to develop a mathematical framework that could accurately quantify oscillation characteristics that emerged as solutions not only by solving flow-oriented equations but by the original application of oscillator equations. Transport processes occurring between the successive stages of a transportation network are described as interactions of a coupled oscillator network. This approach makes it possible to analyze vast transportation networks within the rich modeling phenomenology on synchronization. Besides the introduction of novel techniques in transport analysis, another important research question considered in this study was under which conditions, a synchronous operating point existed on the network parameters and topology. The development of mechanisms for the analysis, evaluation, and control of dynamic synchronization in transport networks enables their effective control. In particular, we investigated the effects of variations in transport period offsets and transport delays between milk-run suppliers to improve the planning of vehicle routing. In addition, a just-in-sequence (JIS) transportation network was studied to investigate the crucial trade-off between transport delay, transport period offset, and coupling strength. A new transport control mechanism was thus developed to improve the coherence of a JIS supply process.

The rest of this article is organized as follows. In the next section, we first discuss the importance of transport synchronization in general and analyze the relevant literature with respect to transport synchronization and/or the application of an oscillatory approach to solve transport management problems. Then, we map transportation networks by using a modified Kuramoto model in which synchronization can be well described and better understood within an established nonlinear dynamics framework. In the following section, we discuss two real-world examples from the automotive industry and show how the new approach can be successfully applied. The last section contains our conclusions and discusses some directions for future work.

2 | LITERATURE REVIEW AND PROBLEM STATEMENT

A very early field of research on synchronization and stability in transportation networks was traffic theory. Bavarez and Newell (1967) evaluated a street network for determining the total delay and the total number of stops for several types of signal coordination schemes. They found that for any given common cycle time and given splits at each intersection, there is a choice of phases that simultaneously minimizes both the total delay and the total number of stops. In the

following decades, the topic of traffic dynamics inspired a large number of publications with increasingly sophisticated methods of nonlinear dynamics. In general, nonlinear models can generate more realistic traffic oscillations, but they make the analytical quantification of the oscillation characteristics more difficult.

Vehicle routing constitutes a further interesting area for synchronization and stability issues. Drexler (2012) presented an extensive survey of vehicle routing problems with multiple synchronization constraints. In addition to the classical synchronization problem of vehicle routing (which vehicle visits which customer), further synchronization requirements between the vehicles, concerning spatial, temporal, and load aspects were covered. A classification of synchronization was introduced for the interdependence problem between vehicle routing where task, operation, movement, load, and resource synchronization had been identified.

In general, synchronization can be considered an intrinsic problem of transportation management. The orchestrated combining of transport resources such as trucks, trailers, or drivers is key to improve the overall supply chain performance. Synchronization problems do not only apply to the classical truckload shipments. Public transport that minimizes the interchange waiting and delay time of all passengers by schedule synchronization is a further interesting area of research (Ibarra-Rojas & Rios-Solis, 2012; Kang et al., 2016; Wong et al., 2008). There are many related areas with similar coherence issues. Some examples are service operations (such as home cares), forestry applications, cooperating technician teams at customer locations, or snow plowing operations and road marking (Tilk et al., 2018). Independent of a concrete application problem, transport delays are inevitable and pervasive in a transportation network, causing synchronization problems, fluctuating or excessive inventories, and lack of robustness of inventories against cyclic perturbations (Sipahi et al., 2009). Blumenfeld et al. (1991) analyzed the trade-offs among transportation, inventory, and production set-up costs and demonstrated that synchronizing production and transportation schedules generates sufficiently large cost savings. Here, sometimes, the shipment frequency can be more significant than the length of the transit period, which stresses the importance of the regularity of transport intervals and their interactions in different synchronization states (Baumol & Vinod, 1970). A synchronized transport process influences not only the costs but also the service level (Tawfik & Limbourg, 2019). Nevertheless, it is generally very challenging to find an optimal trade-off between transport services and transport costs that respect all operating constraints (He et al., 2019).

The synchronization phenomena and synchronous behaviors of complex oscillatory networks have been widely studied. However, there are relatively few investigations in the field of supply or transportation networks. In his study, Dunbar (2007) considered the problem of the distributed control of dynamically coupled nonlinear oscillators. Supply chains

were mentioned as a potential area of application without a discussion on a deeper supply chain management context. Gan and Wang (2013) investigated synchronization problems for a class of supply chain networks that have nonlinearly coupled identical nodes as an asymmetrical coupling matrix. Both supply chains and synchronization were analyzed on a general level without any specific references to transportation networks. Synchronization and chaos control in supply chains were investigated by Göksu et al. (2015). Linear feedback controllers in combination with the Lyapunov stability theory were used to verify the robustness of the proposed synchronization and control methods. A more specific application in the control of material or traffic flows in networks by using phase entrainment was presented by Lämmer et al. (2006). They showed that, under certain assumptions, the control of nodes can be mapped to a network of phase oscillators and illustrated the method using an example of traffic signal control for road networks. Material flows in production systems were mentioned as a possible area of the application of the proposed concept. Helbing et al. (2004) described supply networks as a physical transport problem with the help of balance equations for the flows of products and for the adaption of production speeds. They conducted a stability analysis by linearizing the model equations, which generated a coupled set of second-order differential equations. These equations could be interpreted as a set of equations for linearly coupled damped oscillators. With the help of this oscillatory model, the bullwhip effect could be described as a connective instability that corresponds to resonance effects. This study by Helbing et al. (2004) is the first description of generic oscillators for supply networks. On the basis of this work, Donner et al. (2007) and Donner (2008) studied a decentralized control approach for the regulation of intersecting material flows within a transportation network. It was shown that the presented control approach leads to phase entrainment, which allows one to optimally use the available transportation capacity of the network. They found that the network performance and the degree of phase entrainment are closely related to each other. Although Donner (2008) discussed the Kuramoto model for the degree of phase entrainment, the main study of phase synchronization was not based on a generic oscillatory model, where oscillators were explicitly modeled. The solutions were generated using flow-oriented balance equations for the temporal evolution of the input and output material flows. Xiao et al. (2016) investigated the day-to-day evolution of network flows from travelers' route choices and their learning behavior on the perceived travel costs. An analogy to a damped oscillatory system was used, and a stability analysis was performed. Important features such as damping ratio, angular frequency, and the obedience to the minimum total potential energy principle were used to determine the oscillation pattern. It was found that energy decreases as travelers stay on their current routes, which is analogous to the damping of an oscillator. Klug (2022) recently published an oscillatory model for supply chains. Two coupled van der Pol oscillators

were used to model and control the dynamical interaction of an inventory system.

Summarizing our literature review, we have found very few examples of the application of a generic oscillating model in transportation science. These were either generally designed for supply networks (Donner et al., 2007; Helbing et al., 2004) or very specifically (Xiao et al., 2016) for the consideration of travelers' choice decisions or inventory control (Klug, 2022). Therefore, our goal was to develop a general approach for the evaluation of the synchronization phenomena to support the planning and operation of transportation networks.

3 | TRANSPORTATION NETWORK MODEL (MATHEMATICAL FORMULATION)

The modeling of transport processes has a long tradition in the field of operations research and quantitative modeling. Here, a broad field of analysis spans from classical transportation scheduling (Kelley, 1955), transportation cost minimization (Evans, 1958) to diverse model extensions (e.g., Balachandran & Perry, 1976; Glover et al., 1974) to current problems such as electric vehicle charging networks (Chen et al., 2021). In principle, although there are transport models with extended application areas (e.g., linear programming), each model is used with respect to specific questions to be answered. The oscillator model described in the following represents a model with a limited range of application and aims exclusively at the dynamic analysis of synchronization processes in transportation networks. Due to the size and application focus of transport network synchronization, an emergent model was used (Vaario & Ueda, 1998). Although the individual transport process is only reduced to the very simple time sequence between the start and end of the transport, this makes it possible to describe large networks in emergent synchronization behavior. The goal of the study is not the individual evaluation of transport processes, but to obtain information about the complex synchronization dynamics of different network topologies.

3.1 | Model building and validation

To analyze and evaluate synchronization and stability issues, we modeled transportation networks by using coupled oscillators. The oscillatory methods used in this study constituted oscillatory elements coupled with each other in a system. Each node of the transport network vibrated according to its transport frequency, induced by its transportation network partners (see Section 3.2). This dynamic representation of a transportation system, whether it involves roadways, railways, sea links, airspace, or intermodal combinations, allows one to model various topological attributes of a transportation system (Zhang et al., 2015). The transportation network model was mapped and validated in a real-world setting based on the existing inbound supply networks of a large German

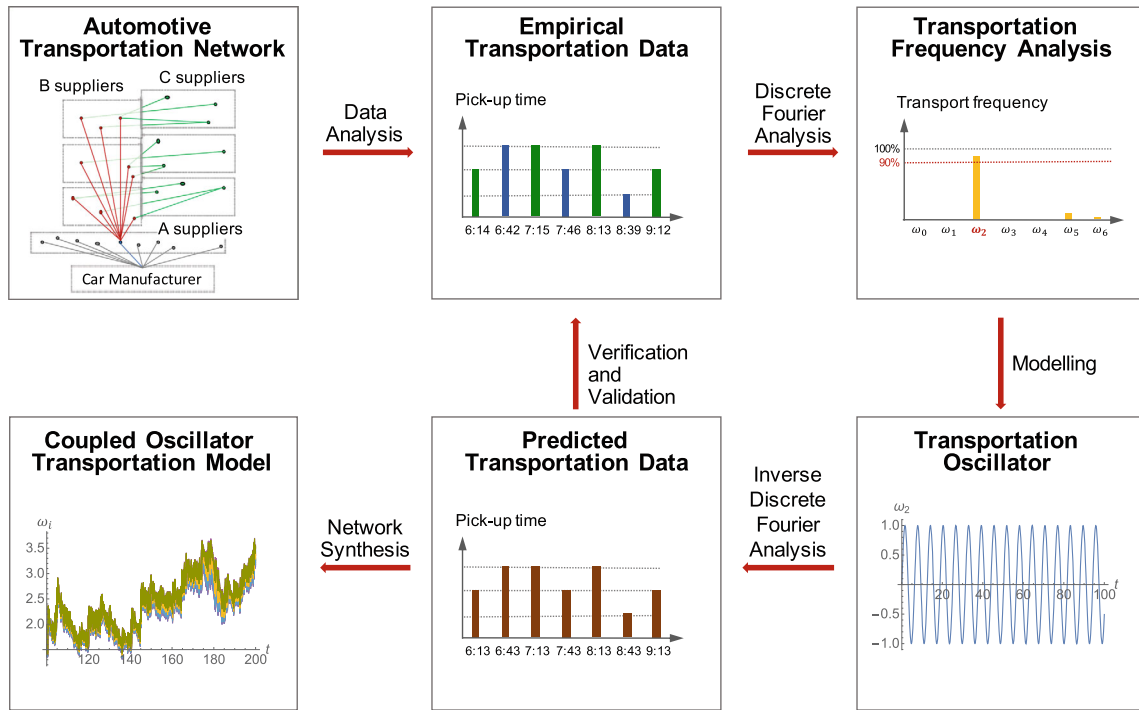


FIGURE 1 Model building process

car manufacturer (see Section 4). The starting point for the modeling of transport oscillators as the elementary building blocks of a transport network was the empirical acquisition of the transportation time-series (see Figure 1).

The data core of the time-series generation was the actual loading and unloading times of the respective freight relations examined for the period under investigation (see Section 4). Because of the real-time scanning processes of all the containers loaded and unloaded by the truck driver in combination with a tracking and tracing system used throughout for vehicle control, all transport processes could be recorded and tracked to the minute. With the application of a Fourier transform, each time series could be transformed into simple sinusoidal oscillations, building the basis of the transport frequency parameterization of suitable transport oscillators. The basic problem that arose upon the use of real discrete transport data was their non-equidistance, which was assumed when using discrete Fourier transforms. By using a linear interpolation technique, the non-equidistant problem could be transformed into an equidistant (uniform) problem by resampling, which could then be analyzed using a discrete Fourier transform (see Appendix A). A discrete Fourier analysis generated a typical transport frequency spectrum when the time signal was transformed into the frequency signal. The main frequency for the respective oscillator model was selected using the relative amplitude components of the frequencies. This main parameter of the model validation with a threshold value of 90% of the relative amplitude (for all direct shipping) allowed a transport process affine mapping of the corresponding real transport processes (see ω_2 in Figure 1). High- and low-frequency components resulting from the small deviations in the main transport process were thus filtered out.

With the help of an inverse discrete Fourier analysis, the original input signal could be recovered and validated with the described relative amplitude evaluation. After the analysis and validation of all of the individual oscillators involved in the transport network, their subsequent combination into an oscillator transportation model was performed.

3.2 | Coupled oscillator transportation model

The core elements of every transport system are individual physical transport processes. An important descriptive criterion of each transport process $i = \{1, \dots, N\}$ is its transportation time T_i , which is the time difference between the end of transport at the destination point and the start of transport at the source. The transport process can be mapped using a phase model in which a phase angle θ_i describes the current temporal transport state. The phase angle θ_i measured in radians starts at 0, then passes through a transport period and ends at 2π (see Figure 2). Repetitive transport processes can thus be described with the help of the time oscillation of a phase angle. The phase angle θ_i and its angular frequency ω_i are determined by the transport time T_i according to $\theta_i = \omega_i = 2\pi/T_i$.

Each transport process can thus be described with the help of an oscillator in which the physical transport time T_i is converted into a transport (angular) frequency ω_i . Transport oscillators represent the dynamic evolution of a transport process with the help of a scalar phase coordinate, which describes the current and instantaneous transport state. Transport processes require a certain organizational time delay δ_i , which results from process-organizational and information-technical procedures in transport planning. Thus,

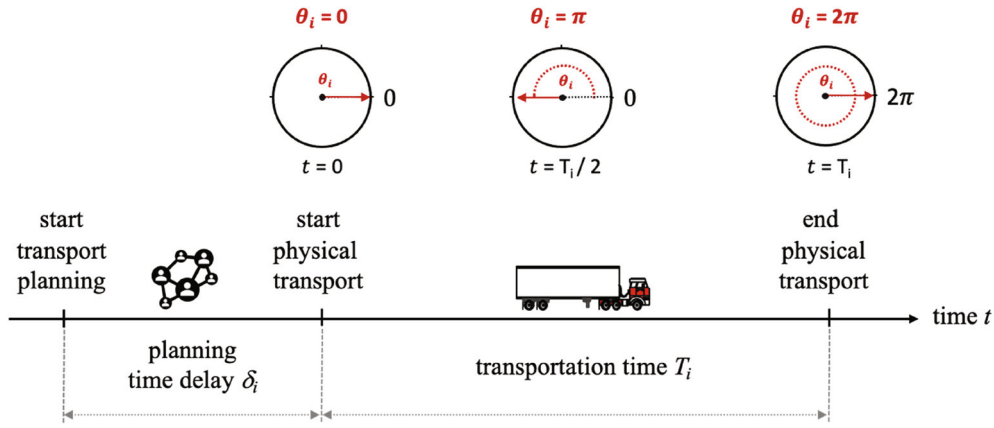


FIGURE 2 Transport process system parameter

lead times caused by decision making, communication processes, and organizational interfaces are translated into the planning time delay δ_{ij} between shipment i and j , representing its adaption time.

Modeling transportation networks are characterized by a population of N heterogeneous transport oscillators with continuous, bidirectional, and antisymmetric coupling. The transport network topology and coupling strength among the oscillators are mapped to a connected, bidirected, and weighted graph $G(\mathcal{N}, \mathcal{E}, \mathcal{A})$ with nodes $\mathcal{N} = \{1, \dots, N\}$, edges $\mathcal{E} \subset \mathcal{N} \times \mathcal{N}$, and coupling matrix \mathcal{A} with the elements $a_{ij} \geq 0$. This graph-based modeling allows one to analyze and simultaneously represent any real transport network in a compact and general form. In this study, a modified and extended version of the generic Kuramoto model was applied (Kuramoto & Arakai, 1984), where the transportation network is represented by a set of N coupled differential equations:

$$\frac{d\theta_i}{dt} = \omega_i + \sum_{j=1}^N a_{ij} \sin(\theta_j(t - \delta_{ij}) - \theta_i(t)), i \in \{1, \dots, N\}. \tag{1}$$

In the Kuramoto model, the temporal variation of the phase angle $\dot{\theta}_i$ and thus the transport time of each transport process is described in terms of intrinsic and extrinsic components. Intrinsically, each transport process is described by its own transport time or angular frequency ω_i (see above). If one were to consider only a single transport process in isolation (see Figure 2), then the phase evolution would be completely determined exclusively by the intrinsic transport time. In a transport network analysis, extrinsic influences from upstream and downstream transport processes must also be taken into account. Extrinsic network influences are described using coupling strength a_{ij} , mapping different transport relations and connectivity arrangements. According to the bidirectional and antisymmetric coupling of the oscillator network, we could map various transport situations with various typological structures. The coupling strength a_{ij} (a_{ji}) indicates how the transport oscillator j (i) impacts the transport oscillator i (j), describing the different control processes and real

dependencies of successive transport activities. The coupling constant ranges from 0 to 1.0, indicating whether transport i is completely independent or completely dependent on the transport j .

The aim of the study is the dynamic analysis of synchronization processes in transportation networks (see Section 3). Synchronization is represented in the Kuramoto model by the adjustment of different transport periods represented by the sinusoidal coupling function used in (1). This interaction function vanishes when the phases are identical or pull the phases of the individual oscillators together $0 < |\theta_i - \theta_j| < \pi$, or push the phases apart $\pi < |\theta_i - \theta_j| < 2\pi$ (see Chapter 3.3). Transport oscillator i responds to the transport oscillator j with a certain organizational time delay δ_{ij} (see above).

The following modifications to the idealized original Kuramoto model were made, with less restrictive generalizations to better represent the dynamics of collective transport:

- The homogenous Kuramoto model describes coupled oscillators with an equal coupling constant between all oscillator pairs, scaled with the total number of oscillators. The proposed model (1) uses a variable coupling strength a_{ij} , mapping different strengths of the transport relations. Each transport process competes with the connected transport processes to align with its transport frequency. The magnitude of the coupling strength controls this synchronization-enforced coupling.
- Time delays due to time lags in the reaction to transport changes were considered with δ_{ij} .
- The natural frequencies of the Kuramoto model are described by a symmetric, unimodal probability density $g(\omega_i)$, such as a Lorentzian or a Gaussian. Our natural frequencies are only based on the individual transport period T_i of each means of transport and each individual freight relation according to $\omega_i = 2\pi/T_i$.
- The highly symmetrical Kuramoto model assumes that each oscillator i is connected to every other oscillator j in the network (all-to-all coupling) and therefore lacks an explicit spatial topology. By describing the

concrete transport models in the automotive industry, we investigated specific transport topologies, namely, milk-run and just-in-sequence transportation (see Section 4).

With the description of the transport processes using a coupled oscillator network, the following opportunities and advantages arose:

- Important constituent characteristics of a transport process, such as transport duration, coupling with upstream and downstream transports, as well as transport time delays, are mapped in a focused and compact manner in the model.
- Because of the phase representation, real transport processes can be simplified. This enables a comprehensive and global description of the collective synchronization dynamics in large transportation networks.
- The very different phase transitions from synchronized to unsynchronized states with the corresponding rich dynamics can be better understood with a dynamic rhythmic representation of oscillators.

In contrast, the model approach used was based on certain assumptions and limitations:

- The phase reduction approach used represents a simplification of the real transport process. Although this facilitation offers advantages for synchronization planning in larger networks, this approach cannot be used to investigate detailed planning issues in transportation management (e.g., consolidation and tour planning).
- Time delays of transport processes are mapped with a fixed time δ_{ij} , which means that real random processes are only partially mapped. Improvements upon the introduction of stochastic oscillators by adding a random process to the phase are however conceivable.

3.3 | Transport network synchronization and stability

The notion of synchronization lacks a unique interpretation. There is neither a common understanding of synchronization in transportation, nor an accepted way of measuring and quantifying it (Chankov et al., 2014). In our case, synchronization was considered the adjustment of different transport periods represented by phase angles due to the interactions among different transport nodes in a network (phase coherence). The dynamics of the transportation network model arose from a trade-off between the goal of transport collaboration in the supply network and therefore transport synchronization (described by the oscillator coupling) and each oscillator's tendency to align with its natural transport frequency ω_i , representing the individual requirements of each network partner. Intuitively, a weakly coupled and strongly heterogeneous transportation network does not display any coherent behavior, whereas a strongly coupled network with similar natural frequencies is amenable to synchronization. Mapping transport networks with a coupled phase model represents a

simplification; nevertheless, these equations are difficult to analyze in general, as the interaction functions can arbitrarily have many Fourier harmonics (Strogatz, 2000).

The sinusoidal coupling function used in (1) can be thought of as the phase response of oscillator i to the input from oscillator j . This interaction function vanishes when the phases are identical or differ by π , representing phase and anti-phase synchronization. In the neighborhood of the phase identity of $0 < |\theta_i - \theta_j| < \pi$, the sinusoidal values pull the phases of the individual oscillators together (tendency to combine transports), while in the case of the near-antiphase of $\pi < |\theta_i - \theta_j| < 2\pi$, the sinusoidal value pushes the phases apart (tendency to split up transports). In addition to this transient synchronization state, a single attracting synchronous and a single unstable antiphase constellation for pairs of oscillators exist. The proposed dynamics of our chosen phase model supports our objective to investigate different types of synchronization states with its spatiotemporal complexity in transportation networks.

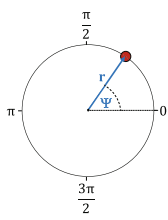
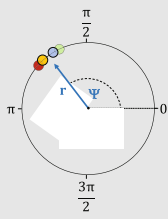
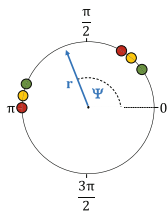
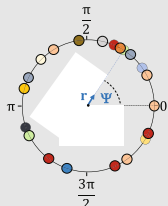
First, it is important to define and distinguish between different phase coherence regimes, which generally can occur in transportation networks. Phase synchronization means that the transport oscillators have a preferred phase relation to each other and that the oscillators adjust their phases as a function of their phase difference. To visualize the different coupling states of the oscillators, we used the following order parameter z_m , which was adapted to our transportation model (Mardia, 1972):

$$z_m = r_m e^{i\psi_m} = \frac{1}{N_m} \sum_{j=1}^{N_m} e^{i\theta_j}, m \in \{1, \dots, M\}. \quad (2)$$

This phasor representation allows one to depict the mean phase ψ_m of the set of N_m oscillators and with the vector r_m to measure the phase coherence of the oscillators for a specific supplier group m . The complex order parameter of the centroid vector r_m ranges from $r_m \approx 1$ (coherence), when the phases of all oscillators become aligned, to $r_m \approx 0$ (incoherence), when phases are uniformly distributed. We measured the time-averaged synchronization order parameter for different supplier groups M and different numbers of suppliers N_m in each supplier group.

Table 1 depicts various synchronization regimes depending on the phase adjustments of the i -th and the j -th oscillator, either for the total network, partially for specific clusters of the network, or locally for the pair-wise interaction of two oscillators i and j . Therefore, all types of regimes could be separated in total, partial, and local synchronization regimes. We started with a total (partial) synchronized transportation network (subnetwork). The perfect state of transportation synchronization was where all the phases θ_i became aligned by converging to a common constant frequency. Therefore, no phase differences between any two oscillators could occur. After the transformation to a rotating frame, this highest level of perfect phase coupling was shown in the phasor representation, where after a possible transient period, only one final phase for all

TABLE 1 Different synchronization and desynchronization regimes

Synchronization regime	Mathematical representation	Phasor representation
Perfect synchronization	$\Delta\theta_{ij}(t) = \theta_i - \theta_j = 0$ Phase difference is 0 at any time t	
1:1 phase locking	$\Delta\theta_{ij}(t) = \theta_i - \theta_j \leq \epsilon, \epsilon \in \mathbb{R}^+$ Phase difference does not exceed a specific threshold ϵ at any time t	
$n:m$ phase locking	$\Delta\theta_{ij}(t) = n\theta_i - m\theta_j \leq \epsilon, \epsilon \in \mathbb{R}^+, m, n \in \mathbb{N}$ Difference in multiple phase ratios does not exceed a specific threshold ϵ at any time t	
Nil phase locking	$\Delta\theta_{ij}(t) = \theta_i - \theta_j > \epsilon, \epsilon \in \mathbb{R}^+$ Difference in phase ratios does exceed a specific threshold ϵ at any time t	

individual oscillators existed on a unit circle in the complex plane (see Table 1 right column). One-to-one phase locking existed if the instantaneous phases of oscillations were locked in a specific ϵ -region, which could be measured by the time evolution of the phase difference. Despite different frequencies, it was possible for the phase ratios n and m to be locked and to not exceed a specific threshold ϵ . By varying the ϵ -region, one could differentiate between stronger and looser locked transportation networks. In the case of nil phase locking all individual transport oscillations added incoherency, and no macroscopic rhythm was produced, as indicated by a phasor representation, where all the phases were randomly scattered around the unit circle.

We were particularly interested in the phase transition from the synchronized to the unsynchronized states. When the spread of natural frequencies $\Delta\omega_i$ was larger than the coupling a_{ij} , the transportation network behaved incoherently, with each oscillator running at its natural frequency. Upon the reduction of the frequency spread and/or an increase in the coupling strength, the incoherence persisted until a certain threshold was reached. At this phase transition point, some of the oscillators started synchronizing, while others remained incoherent (Strogatz, 2000). It was obvious that the network topology had a strong effect on the dynamics,

and therefore, the phase entrainment transitioned. This is the reason why it is important that existing general studies on the synchronization and stability of oscillating networks are supplemented by concrete empirical applications for specific network topologies.

4 | AUTOMOTIVE TRANSPORTATION NETWORKS (EMPIRICAL STUDY)

To show how the synchronization analysis for transportation networks could be applied to a real-life problem, we analyzed and evaluated the issues of transport synchronization and stability in the automotive industry. Our goal was to find stabilization strategies for the planning, operation, and control of transport processes in two different transportation network topologies. By mapping a ring topology with delayed coupled oscillators, we could model a milk-run transportation network. The second topology was a classical hierarchical tree network structure related to the inbound part (in relation to the car manufacturer) of a just-in-sequence transportation network. Our research focus was the synchronization dynamics of the existing inbound network structures in the automotive industry. For further investigations, we selected these two transportation networks for the following reasons:

- The topologies represent two main inbound supply chain network types from a car manufacturer's point of view (OEM, original equipment manufacturer), widely spread in the automotive industry.
- These partial networks show the maximum intra-interaction within the network and the minimum inter-interaction among the subnetworks.
- These network types can be found in a variety of other application areas, allowing the analysis results to be transferred to other industries.

The distance to the supplier and the transport volume were the main criteria for the selection of a specific transport concept and were therefore used as the main separation criteria. Therefore, all the suppliers involved in the inbound transportation process were separated according to the transport volume and their geographical distance from the automobile manufacturer's assembly plant. Three different transportation areas with regional (less than 50 km), national (located in Germany), and international (located outside Germany) suppliers were used. In addition, the transport volumes were divided into three classes: A-supplier (more than one FTL per week), B-supplier (less than one FTL per week), and C-supplier (general cargo with sporadic delivery). The freight volume was always calculated in relation to the inbound transport volume of the car manufacturer. Clustering the empirical data by the transportation distance and volume allowed us to map internally similar transportation processes within the group while accounting for heterogeneous differences between groups in terms of the synchronization of transportation processes.

Our coupled oscillator model was mapped and validated in a real-world setting based on the existing inbound supply networks of a large German car manufacturer. All the parameters used were based on the empirical data of the used transport management systems (TMS), combining a range of different transport-relevant information.

For the analysis of milk-run transports, 12 milk-runs in Bavaria were initially examined, with Milk-Run 10 selected for a more intensive data analysis and analyzed in more detail with respect to the synchronization behavior. Therefore, a large amount of road transport data from the used transportation management systems (mainly real-time vehicle arrival and departure times over a period of 1 year) were evaluated. The just-in-sequence transport analysis was based on 12 regionally based JIS suppliers, all of which were located less than 50 km from the vehicle plant. For the subsequent synchronization and stability analysis of the entire JIS network, the data (e.g., real-time truck tracing, loading, and unloading times) were evaluated over a period of 1 month.

All stochastic quantities for the transport periods, transport frequencies, and coupling strengths were represented in the empirical studies by using truncated normal distributions. For each transport topology, the transport network was first described, and then, a synchronization and stability analysis was performed.

4.1 | Milk-run transportation

4.1.1 | Transportation network

On a milk-run transport, shipments from several middle volume suppliers (B-freight supplier) are consolidated and transported directly to the OEM cross-docking facility. The main prerequisite is relatively stable production call-offs and therefore transport volumes, which only enables a high freight capacity utilization. With groupage round-trip transports, the partial loads of a manageable number of geographically concentrated suppliers are picked up sequentially and periodically and put together to form a complete load. During a round-trip, a successive exchange of empty containers for full containers takes place. In the milk-run, the truck with the required empties starts from the cross-docking facility of the vehicle manufacturer. The individual suppliers of the round-trip are successively approached. At each stop, the empty containers requested by the respective supplier are unloaded, and the full containers are loaded onto the truck. After the processing of the last supplier, all the empty containers have been unloaded and, ideally, a complete load of full goods has been generated, which is then transported to the OEM cross-dock. The consolidation of the partial loads into complete loads reduces freight costs and increases the delivery frequency as compared to individual deliveries. At the same time, goods receipt capacities and processes can be better planned, as truck deliveries to the OEM are regularly made at predefined time periods.

For our empirical study, we investigated a milk-run with four regional suppliers (A to D). In the first step, the delivery routes and the sequence of servicing the suppliers are fixed. All milk-run trucks are handled via an inbound cross-dock site in the immediate vicinity of the vehicle plant. Pick-up (supplier) and cross-docking times must be scheduled in accordance with the car manufacturer's central transport planning system (TPS). Depending on the weekly material call-offs, predefined cycle times were calculated for the round-trips, which resulted in a transport period of $T_{\text{OEM}} = 7.85$ h for our observation period (see Table 2). Because of the short-term (less than 1 week) changes in the vehicle program, transport quantities, and their composition were subject to continuous fluctuations. The empirically recorded transport periods T_{RMS} for the milk-run suppliers showed a mean value of 7.81 h and a standard variation of 0.80 h. These transport time fluctuations were caused by varying traffic situations and loading times depending on the daily delivery quantity (full and empty containers). All the milk-run transports were carried out by a carrier. There was a pool of trucks available to run the round-trip service between the suppliers and the manufacturer (12 milk-runs in total). The carrier was provided with transport orders to schedule the collection dates and times. Various regional, national, and international C-suppliers delivered the sub-components to the milk-run suppliers. The increasing mean transport periods ranged from 67 to 204 h with increasing standard deviations (18 to 177 h).

TABLE 2 Number of suppliers, transport period, and transport frequency distributions (mean; standard deviation)

	OEM	Regional milk-run supplier RMS	Regional C-supplier RCS	National C-supplier NCS	International C-supplier ICS
Number of suppliers		4	11	27	45
Transport period T_i (h)	7.85	(7.81;.80)	(67.2;18.0)	(153.6;85.0)	(204.0;177.0)
Transport frequency ω_i (h^{-1})	.80	(.80;.08)	(.09;.03)	(.04;.02)	(.03;.03)

TABLE 3 Matrix coupling strength a_{ij} distributions (mean; standard deviation) above and time delays δ_{ij} [h] below.

From	To							
	OEM	A	B	C	D	RCS	NCS	ICS
OEM		(1.0;.0) .55						
A			(1.0;.0) .55			(.03;.01) 24	(.02;.01) 48	(.01;.01) 168
B		(1.0;.0) .55		(1.0;.0) .55		(.03;.01) 24	(.02;.01) 48	(.01;.01) 168
C			(1.0;.0) .55		(1.0;.0) .55	(.03;.01) 24	(.02;.01) 48	(.01;.01) 168
D	(1.0;.0) .55			(1.0;.0) .55		(.03;.01) 24	(.02;.01) 48	(.01;.01) 168
RCS		(.003;.001) 1	(.003;.001) 1	(.003;.001) 1				
NCS		(.002;.001) 1	(.002;.001) 1	(.002;.001) 1				
ICS		(.001;.001) 1	(.001;.001) 1	(.001;.001) 1				

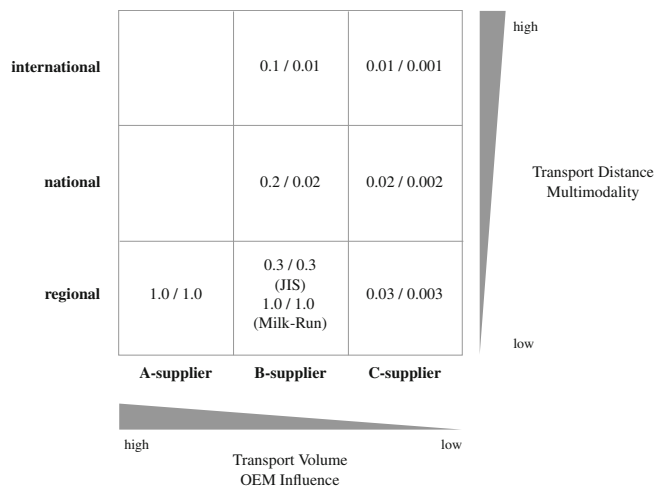


FIGURE 3 Coupling strength a_{ij} (first value) and a_{ji} (second value) matrix

The importance and the strength of the connection of each individual transport within the respective transport system considered is described by the coupling strength a_{ij} in the oscillator model (see Section 3.2). The basis for the quantification of the coupling strengths (see Tables 3 and 6) was formed by our own recent investigations in the transport network of a large German automotive manufacturer as well as long-term investigations in the field of transport management in the automotive industry (Klug, 2018).

Figure 3 lists the transport coupling strengths between the OEM and its suppliers (first value) and vice versa (second value) used for the following simulation runs. The

transportation network under study was predominantly dominated by the vehicle manufacturer. In addition, supplier-side problems and transport optimization by carriers influenced the transport behavior of the suppliers in the other direction, although these were largely driven by OEM specifications. This dominant pull effect of the OEM on transportation dynamics was expressed by a tenfold increase in the OEM-supplier transport coupling strength (see Figure 3). The main driver of the call-off and the delivery volumes handled was the vehicle manufacturer’s master production schedule. This determined the total inbound transport volume and frequency. The strongest coupling ($a_{ij} = 1.0$) was present when a transport failure led directly to a delivery delay at the OEM. This was the case for direct transports, both for the milk-run via the respective B-supplier (see Section 4.1.2) and for the just-in-sequence delivery via the A-supplier (see Section 4.2.1). A delay in the loading or transport process directly affected the inbound material flows at the OEM’s goods receiving. The supplier integration and, thus, the contact and influence of the OEM steadily decreased from the regional A-supplier to the international C-supplier. While important 1-tier A-suppliers were closely linked to the vehicle manufacturer in terms of the transport technology within the framework of minute-precise just-in-sequence transports, international C-suppliers played a subordinate role in transport planning. Transport structures in the automotive industry, as in other industries, are also highly dependent on the supplier location and delivery volume. Suppliers located

upstream in the supply chain therefore deliver and transport less freight, which decreases the linkage strength. The transport volume shows the same effect. While full loads in direct transport have a massive influence on the inbound transport activities of the vehicle manufacturer, this influence decreases for the B- and C-suppliers with decreasing transport volume. An international C-supplier handles the low delivery volume via a multimodal network. Here, general cargo is consolidated by the forwarder, so that the individual freight only makes up a small part of the total transport volume, which is reflected in a low coupling constant. In general, the coupling strength from regional A-supplier to international C-supplier decreases (see Figure 3).

Specifically, the following evaluation criteria were chosen for the milk-run system under investigation. A regionally based milk-run supplier delivers exclusively for the local OEM and is therefore completely dependent. Milk-runs are round trips in which all transport processes from the automobile manufacturer via the suppliers to the OEM cross-docking facility are sequentially linked (see Figure 5). Therefore, disturbances have an immediate effect on the subsequent transport stages, which are mapped with the highest coupling strength of 1.0 for all the partners of the milk-run transport (see Table 3). The carrier uses a track and trace system (T&T system), which allows the transport information to be updated with an organizational time delay of 33 min ($\delta_{ij} = .55$ h). In a customer-oriented delivery system, the orders of the milk-run suppliers (from milk-run supplier to C-suppliers) determine the transport volume, and the C-supplier has, apart from very rare delivery bottlenecks, only a minimal influence on the delivery and thus, on the transport volume (from C-suppliers to milk-run suppliers). Delivery and transport period adjustments for C-suppliers can be made on average daily (for regional suppliers), every 2 days (for national suppliers), or weekly (for international suppliers). If delivery and transport conditions change, all C-suppliers must notify the milk-run supplier immediately (organizational time delay of 1 h).

4.1.2 | Synchronization and stability analysis

All the simulation runs were carried out over a period of 1 week. Figure 4 depicts the synchronization levels, which are marked by different color classes, divided into the corresponding supplier groups. This transportation synchronization matrix is a compact visual representation of all the phase coherence vectors r_m (2). It provides an overview of the degree of synchronization between the transport processes in the entire transportation network. General simulation results for the milk-run network show a high phase entrainment level for all the four suppliers involved. The milk-run is operated at a very high synchronization level, which is indicated by a high centroid vector $r_{MR} = .88$. A comparison of the mean transport periods with the standard deviations in Table 2 shows a high level of transport reliability. Milk-run transports are restricted to a very tight time window. Regional round-trip

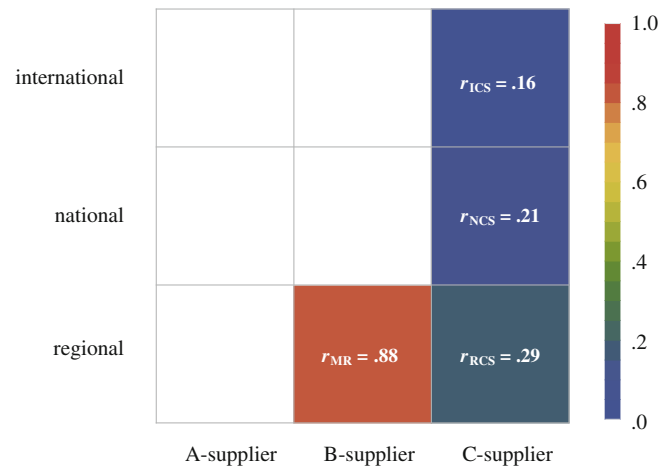


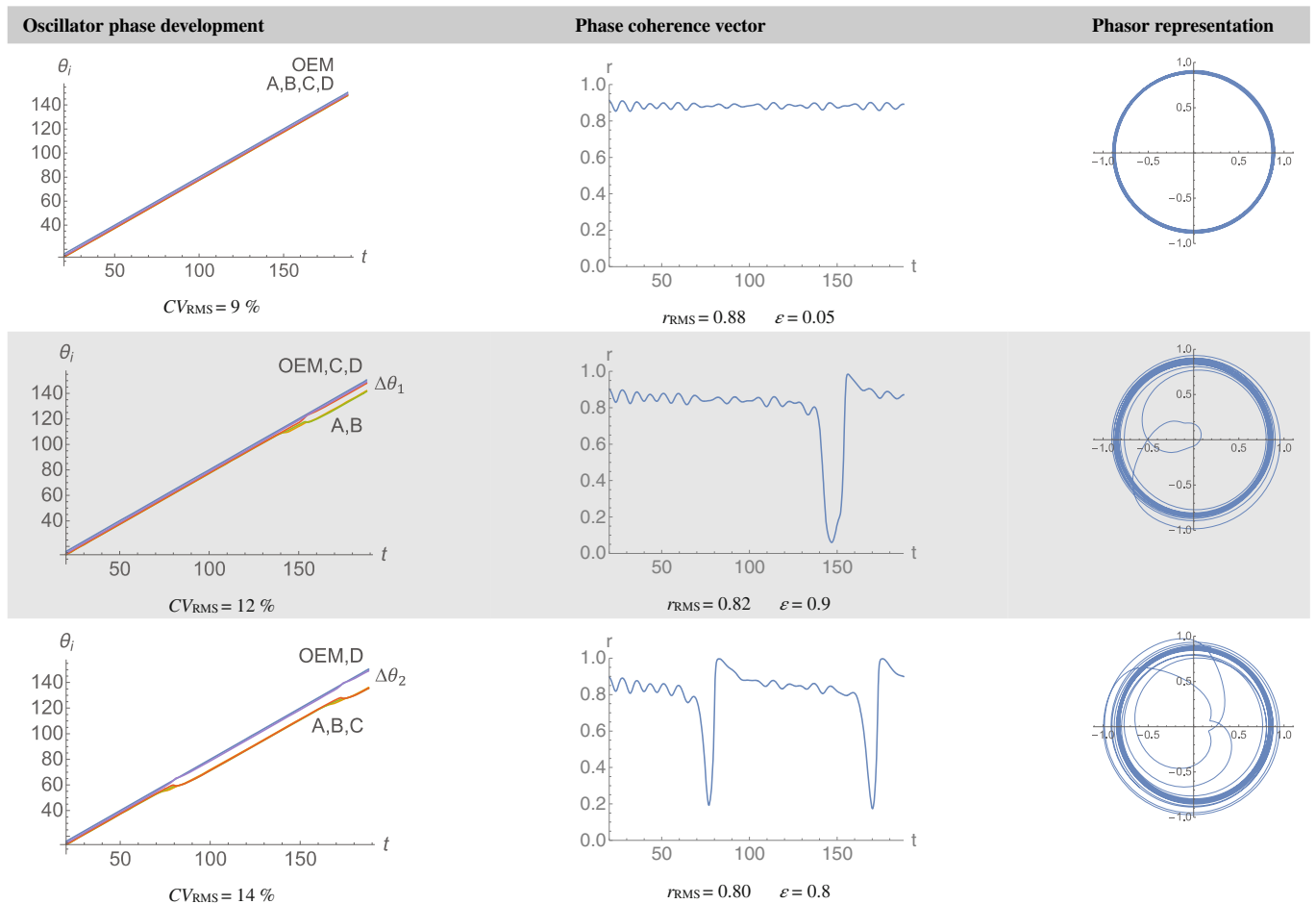
FIGURE 4 Milk-run transport synchronization matrix

transports with only four suppliers guarantee a high schedule and time discipline with a coefficient of variation of only $VC_{MRS} = 9\%$. The synchronization level of the C-suppliers is at a relatively low level because of the increased transport period offsets (between 2.8 and 8.5 d) and the lower coupling strength, so that the phase coherence decreases slowly from the regional (.29) to the international suppliers (.16). In general, it can be observed that the greatest synchronization occurs when the collective mean of the coupling strengths of the oscillators is large and the collective variance of the transport frequencies is small.

To investigate the stability of the milk-run transport network, we analyzed two major factors influencing synchronization, namely, the transport period offset and the delay time of the transport information. First, we investigated the effect of the transport period offset, which is defined as the transport period difference among the individual milk-run suppliers in relation to the predefined OEM trip cycles according to the weekly targets. The main research question was to determine the extent to which the transport periods can be varied without losing the synchronization of the milk-run. If the individual partial transports between the milk-run suppliers are no longer synchronized, the time window for goods delivery in the vehicle manufacturer's cross-dock can no longer be kept, which can delay the subsequent transports in the next shift. We gradually increased the transport period offset, calculated with the coefficient of variation, and started with 9% for the current round-trip plan (see Table 4).

An increasing transport period offset from 9% to 14% reduced the total phase coherence r from .88 to .80 (see Table 4). The phasor representation (2) does show how synchronicity is gradually declining (see right column at Table 4). According to the strong coupling among all the milk-run partners, and the low variations in transportation times, all the phases converged and aligned very quickly for the 9% case. Here, the dominant OEM's transport period strongly coincided with the round-trip periods. This phase locking with a low ε -threshold guaranteed a smooth daily transport process for the car manufacturer. This process of self-synchronization

TABLE 4 Comparison of time development and phase coherence for $t = 168$ h (1 week) for Milk-Run 10



corresponded to the fact that small time fluctuations in the transport sub-processes could be compensated, in spite of the variations in the individual transport frequencies of milk-run suppliers. This was how the milk-run was actually processed without any major disruptions. With a variation of 12% in the transport periods, the synchronous phases were initially guaranteed. At the time of 140 h, the phases of suppliers A and B decoupled after a transition period of 17 h, while suppliers C and D were still bound to the vehicle manufacturer with respect to their transport frequencies. Applied to the daily round-trip transports, this meant that individual fluctuations in the partial transport routes could no longer be compensated and the overall synchronization of the milk-run worsened. Individual measures to accelerate or slow down partial activities (such as loading and unloading, docking, and travel time) were no longer sufficient to maintain the specified round-trip time. A comparison of the phase decoupling showed that a phase splitting $\Delta\theta_1$ by approximately $t = 157$ h took place, so that the specified time window for delivery in cross-dock could not be kept. A further increase in the transport period offset inevitably led to further phases decoupling with decreasing round-trip coherence.

The threshold value of 10.8% offset was used to calculate the permissible deviations of the transport period for milk-run transports, so that the round-trip synchronization

remained guaranteed. In principle, a distinction is made between static and dynamic milk-runs. In a static milk-run, the same suppliers are always served in fixed cycles, with a fixed route and constant delivery volume. If the transport conditions are stable, fixed routes can be put together and run at fixed frequencies. In order to generate collective round-trips despite variations in the call-off and thus transport quantities, it is sometimes necessary to react flexibly with dynamic milk-runs. The calculated threshold of 10.8% translates into an allowed maximum deviation of transport periods of 51 min according to the OEM round-trip time of 7.85 h. This allows variations either in the number of loading quantities or in the maximum geographical range of a possible additional supplier without losing the synchronicity of the round trip. Figure 5 depicts all the milk-run options that could be realized considering the spatial, temporal, and load aspects for the daily milk-run planning (Milk-Run 10).

According to the geographical distance, which was reflected in the varying transport times, supplier A, C, and D could be replaced by another supplier A*, C*, or D*. These suppliers were located in the geographical round-trip area and acted as a possible substitute. In the vehicle routing planning of Milk-Run 10, it was possible to exchange one supplier in the regional environment at a time. Replacing supplier A (C) with A* (C*) resulted in an extended travel time of 23 min

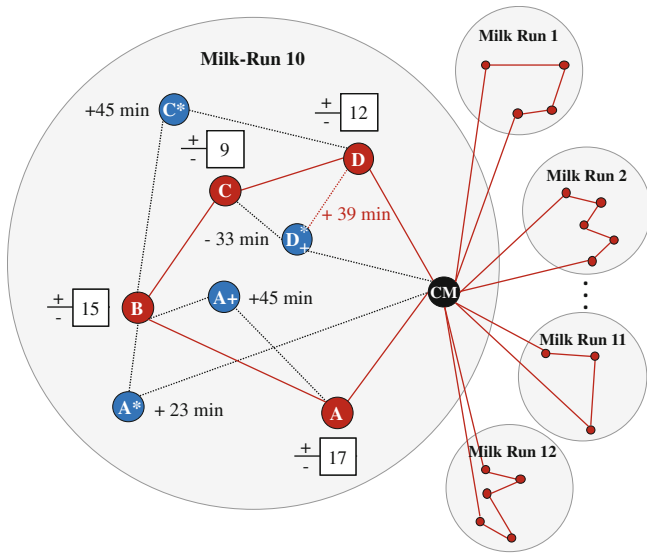


FIGURE 5 Milk-run vehicle route planning

(45 min) because of the longer transport distance between cross-dock CM (B) and supplier B (D). For supplier D, the transportation time was reduced because of a more favorable geographical location between supplier C and cross-dock CM. These three substitute suppliers A*, B*, and C* fulfilled the conditions of a stable and equal transport volume corresponding to that of the respective substitute supplier, so that only these could be considered the geographical exchange partners for Milk-Run 10.

A further option for the vehicle route planning was to add a supplier, when the total transport volume for a round-trip was too low. This added an additional round-trip time of 45 min for supplier A+ or 39 min for D+, which was the same supplier as for the replacement option before. Besides changing the truck route, a variation of the loading volume was possible. Due to the fact that each supplier delivered different parts in different bins, the volume of full and empty containers that could be handled according to the time threshold was different. The total variation of each handling volume was indicated in the +/- box next to each core supplier. The calculation of phase decoupling and thus the synchronization behavior of different transport period offsets in a milk-run thus becomes a valuable analysis tool for the daily vehicle route planning of dynamic milk-runs.

The second crucial parameter to investigate the stability of the milk-run transportation round-trips was the delay time of the T&T system. An important issue to transport control management was the question of how delayed transport information influenced the transport network synchronization. With the help of a parametric (according to δ_{ij}) numerical solution of the differential equations in (1), we gradually increased the delay time of the modeled transportation network from 0 to 20 h. At present, the transport frequencies can be adjusted every 33 min by the carrier, who controls the round-trip accordingly. The loss of synchronicity due to this time delay could be calculated using the differences in r_{MR} between $\delta_{ij} = 0$ h and $\delta_{ij} = .55$ h (see Figure 6). The loss of phase

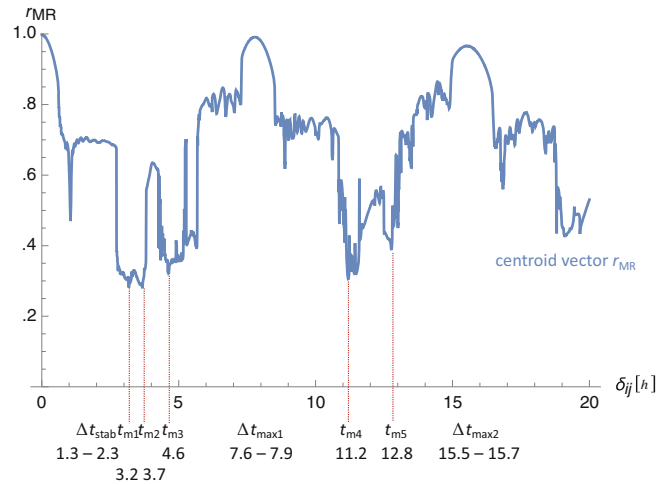


FIGURE 6 Comparison of time development and phase coherence with increasing delay time $\delta_{ij} = 0-20$ h

coherence was calculated for the milk-run with $\Delta r_{MR1} = .22$. Figure 6 shows a high time delay sensitivity, indicated by a strong fluctuating r_{MR} line. After the gradual loss of phase coherence due to the increasing phase offset, the r_{MR} stabilized for a short time on a small plateau ($\Delta t_{stab} = 1.3-2.3$ h) and then dropped to the first and the second relative minimum at $t_{m1} = 3.2$ and at $t_{m2} = 3.7$ h and to the third relative minimum at $t_{m3} = 4.6$ h. After a short transient phase, transport periods suddenly re-synchronized at the maximum plateau level of .99 at $\Delta t_{max1} = 7.60-7.85$ h only to fall back to a lower level with the relative minima at $t_{m4} = 11.2$ h and $t_{m5} = 12.8$. This process was repeated to the second relative maximum of .98 at a time corridor of $\Delta t_{max2} = 15.45-15.7$ h. This cyclical development showed that synchronicity was not automatically lost after a longer delay. If the correct delay time for the transportation control system was chosen, the transport process between the partners in a milk-run could be re-synchronized in a so-called lag synchronization (Rosenblum et al., 1997). Whenever the delay time reached an integer multiple of the milk-run transport period ($T_{RMS} = 7.81$ h), phase coherence occurred. This correlation illustrated very well the necessity to evaluate the synchronized processes with the help of suitable business management procedures (see Section 5). Although we found three relatively equal synchronization maxima, they could only be realized with different processes and with different costs and performance. Figure 6 clearly indicates the nonlinear and nonequilibrium dynamic of a ring transportation topology. Critical time delays (t_{m1} to t_{m5}) had to be avoided. On the one hand, short variations in delay times, sometimes caused by minor organizational or communicational problems, could cause major coupling losses, such as for t_{m1} and t_{m4} where an additional delay time of around 25 min pushed back the phase coherence by up to .45. On the other hand, there was a type of stability islands (Δt_{stab} , Δt_{max1} , and Δt_{max2}), which guaranteed high levels of phase entrainment of up to nearly full synchronization (Δt_{max1} and Δt_{max2}).

TABLE 5 Number of suppliers, normal distributions (mean value; standard deviation) of the transport periods, and transport frequencies

	Regional A-supplier RAS	Regional B-supplier RBS	National B-supplier NBS	International B-supplier IBS	Regional C-supplier RCS	National C-supplier NCS	International C-supplier ICS
Number of suppliers	12	86	101	173	34	44	102
Transport period T_i (h)	(.35;.07)	(50.40;7.56)	(88.80;17.76)	(187.20;123.55)	(74.40;16.40)	(160.80;81.30)	(235.20;188.50)
Transport frequency ω_i (h^{-1})	(18.01;3.74)	(.13;.02)	(.07;.01)	(.03;.02)	(.08;.02)	(.04;.02)	(.03;.03)

4.2 | Just-in-sequence transportation

4.2.1 | Transportation network

JIS delivery is a demand-driven logistics concept, where complete loads are delivered several times a day in sync with the production (Bennett & Klug, 2012). The prerequisite is a high delivery volume with a constant delivery frequency. Because of the degressive freight rates, direct full loads transport represents the most cost-effective transport variant in automotive inbound logistics. This form of transport is suitable for complex, large-volume, and customer-specific modules and components that require late configuration. Typical examples of sequenced delivery volumes are front ends, seats, door panels, bumpers, and headliners. The manufacturer-ordered modules are supplied, in accordance with the sequence call-off, in the same sequence and synchronized with the master production schedules. This schedule-driven JIS delivery uses a centralized approach designed to calculate exactly what is needed. The supplier is producing, sequencing, and dispatching parts exactly in the demanded volume and sequence, according to the car manufacturer's time critical sequence call-off. In this so-called "pearl necklace" system, modules are only produced and pushed through production stages according to a pre-planned production schedule. When the order is fixed (frozen) by the car manufacturer, a bill of materials is broadcast to the module suppliers. Ensuing orders and call-offs together with shipment are processed and then built to a batch of one with a broadcast message some days ahead of when the car is built. Freight forwarders are integrated into the information process and are provided with transport orders including quantities and collection dates and times. Loading and unloading times have to be synchronized because there are only small inventory buffers on the assembly line, which compensate for the slight delays in inbound delivery. At the time of delivery, the trucks drive directly to the unloading point of the vehicle plant and unload containers without delay. The sequence of the part variants in the sequence container corresponds exactly to the removal and installation sequence on the assembly line. In one-to-one exchange, full containers are replaced by the same number of empty containers.

We only focused on the classical just-in-sequence transports, where suppliers were situated in a regional area of not more than 50 km from the OEM assembly plant. Although nowadays OEM assembly schedules are increasingly "frozen" over a period (so-called "frozen-horizon" or "pearl necklace concept") of some days, which gives the supplier more time to react on material call-offs, the sequenced supply can

be accommodated sometimes over substantial geographical distances.

All the JIS transports are handled by shuttle trucks, which run in regular cycles between the supplying and the receiving plant. Narrow time windows are defined for the delivery. The truck docks at the assembly line in the immediate vicinity of the point of need. These docking points are located on the hall wall of the assembly buildings. This enables the implementation of a warehouse-on-wheels concept with two docking stations per delivery point. One docking station with the full container trailer serves as the assembly supply. The resulting empty containers are bundled in the second trailer. If the full-goods trailer is emptied and the empties trailer is also full because of the 1:1 exchange at the workplace, a trailer exchange takes place.

Based on an analyzed period of 1 month, Table 5 depicts the total number of suppliers involved in the JIS transportation network with its transport periods and frequencies.

Just-in-sequence transportation networks are mainly driven by the car manufacturer. The main parameter of a just-in-sequence supply system is the cycle time of the car assembly line. The cycle time is used to synchronize the pace of car assembly with the pace of module supply and delivery of the regional A-supplier. In the short term, this process is defined autonomously by the car manufacturer in terms of its assembly line cycle time and is therefore represented by the high coupling a_{ij} (1) of 1.0 between the OEM and the JIS suppliers. The transport cycles can be adapted flexibly and are always based on the assembly line cycle time of the car manufacturer. To determine the coupling strengths (truncated normal distribution) of the suppliers, the considerations already made for the milk-run were used (see Section 4.1.1). The farther upstream in the supply chain it is, the less influence the car manufacturer has on the master production schedule and the transport planning of the suppliers, mapped with a decreasing coupling strength (see Figure 3 and Table 6). JIS suppliers are directly connected via an EDI system. Every change in the automobile manufacturer's call-off rates is transmitted to the supplier on average every 21 min (see the next section). Delivery and transport time adjustments for B-suppliers can be implemented with an average delay of 12 h (regional), 24 h (national), or 84 h (international) for B-suppliers. In contrast, C-suppliers can adjust their transport processes daily (for regional suppliers), every 2 days (for national suppliers), or weekly (for international suppliers).

TABLE 6 Matrix coupling strength a_{ij} distributions (mean; standard deviation) above and time delays δ_{ij} [h] below

From	To						
	RAS	RBS	NBS	IBS	RCS	NCS	ICS
OEM	(1.0;.0) .35						
RAS		(.3;.1) 12	(.2;.1) 24	(.1;.1) 84			
RBS	(.03;.01) 12				(.03;.01) 24	(.02;.01) 48	(.01;.01) 168
NBS	(.02;.01) 24				(.02;.01) 48	(.02;.01) 48	(.01;.01) 168
IBS	(.01;.01) 84				(.01;.01) 168	(.01;.01) 168	(.01;.01) 168
RCS		(.003;.001) 24	(.002;.001) 24	(.001;.001) 24			
NCS		(.002;.001) 24	(.002;.01) 24	(.001;.001) 24			
ICS		(.001;.001) 24	(.001;.001) 24	(.001;.001) 24			

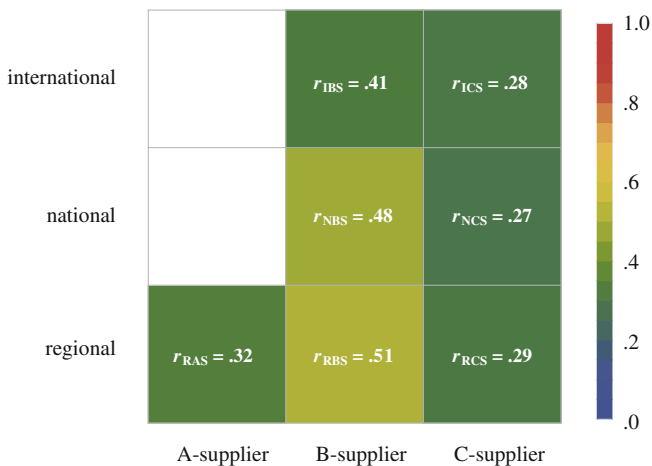


FIGURE 7 Just-in-sequence transport synchronization matrix

4.2.2 | Synchronization and stability analysis

As with the milk-run network, simulation runs were carried out over a period of 1 week (168 h). Figure 7 shows the JIS transport synchronization matrix as a compact and comprehensive representation of synchronization states across the network. The centroid vector r_m (2), which indicated the phase coherence of the specific group of suppliers, decreased during the transition from the regional to the international B-suppliers, while it remained at a low level for all the C-suppliers. A comparison of the mean transport period with its standard deviation in Table 5 showed the considerable diversity of transport relationships. While a regional B-supplier delivered with a mean transport period of 50 h, (standard deviation: 8 h), international B-suppliers delivered at time intervals of 187 h and with a standard deviation of 124 h. In contrast, the long average delivery and transport period of C-suppliers (between 74 and 235 h), combined with the relatively long response times of up to 168 h, did not provide good conditions for phase synchronization.

The relatively low phase coherence of the regional A-suppliers may seem unexpected according to the high level of synchronicity between the car manufacturer and its JIS suppliers. The phasor representation (2) as a mean phase ψ_m of the set of j oscillators for a specific supplier group m was sensitive to the variation of transport time. Although each A-supplier was strongly synchronized with the car manufacturer's production pace, the low value of the centroid vector ($r_{RAS} = .32$) indicates a reduced level of synchronicity, within the group of JIS suppliers. In this specific case, 12 JIS suppliers delivered on average 21 modules according to a batch call-off every 21 min with a cycle time of 60 s of the car assembly line. Each JIS supplier performed with a very low standard deviation per delivery and therefore with a very high phase coherence of nearly 1. In contrast, the supplier group's specific phase coherence with a deviation in transport time of 4.3 min between the individual deliveries was high as compared to the low level of the transport period. Therefore, the variation coefficient of 20% was higher than that of the regional B-suppliers (i.e., 15%).

Figure 8 depicts the phase development across all the supplier groups within 1 week, which was limited to 10 suppliers for better clarity. It is clearly shown that the phase coherence of the individual supplier groups decreased as we moved from regional B-suppliers to international C-suppliers. All the B-suppliers showed coherence periods, where two or more transport frequencies were bound over a specific period of time. Periods of cohesive and non-cohesive phases changed, so that transport processes decoupled and recoupled with each other. The tendency toward one-to-one phase locking (see Section 3.3) was always greater when the dispersion of the transport frequencies was small. The width of the distribution of the transport frequencies reflected the transport heterogeneity of the supply source. B-suppliers showed a relatively low frequency mismatch, indicated by the standard deviation of .01 and .02 (see Table 5). For the 86 regional

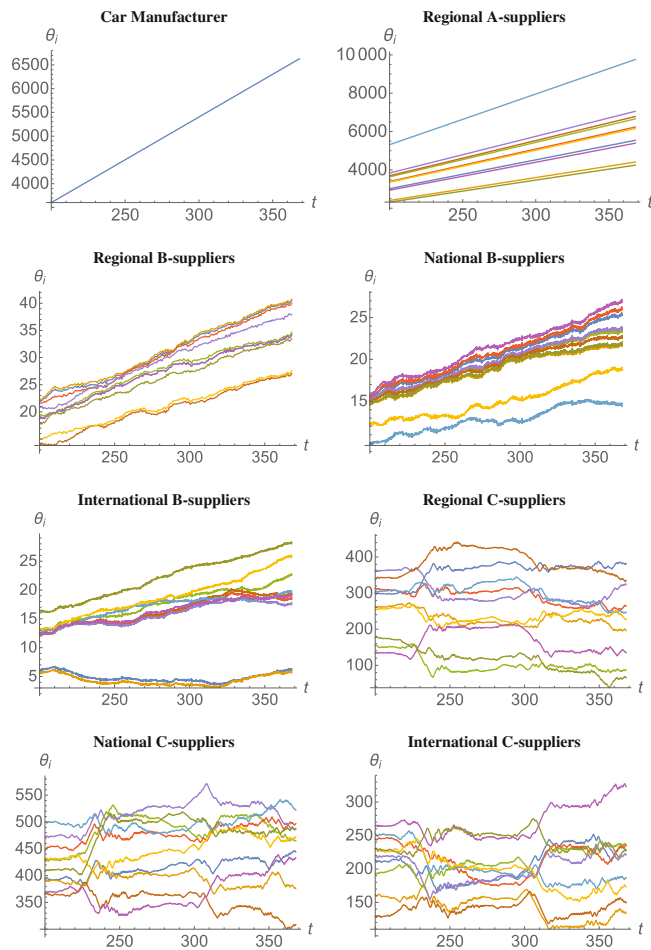


FIGURE 8 Comparison supplier group specific phase development: 10 suppliers per group shown in different colors ($t = 200\text{--}368$ h)

B-suppliers, the standard deviation of 7.6 h compared to a mean transport period of 50.4 h favored the tendency toward phase coupling. Applied to daily transport operations, the probability that shipments from different suppliers would require the same transport processes in the same time window decreased with increasing variation in the delivery times. For all the B-suppliers, the spread of bounded phases from the regional to the international suppliers increased, as the transport periods increased there (see Table 5) and coupling declined from .3 to .1 (see Table 6). All the C-suppliers showed incoherent and randomly distributed transport processes with considerably larger transport periods and delay times. For all the C-suppliers as well as for two international B-suppliers (the two lower ones), the phase development and, thus, the dynamic development of transport processes were largely decoupled from the specifications of the automobile manufacturer (indicated by a significantly different θ). This situation corresponded to the fact that the demand-driven transport concept in a JIS network, starting from the automobile manufacturer, was lost upstream in the supply chain. On the one hand, the longer delivery and transport time adjustments (between 1 day and 1 week) and transport periods (between 74.4 and 235.2 h) for the C-suppliers prevented a quick reaction to the changes in demand. On the other hand,

the transportation synchronization was correlated to supplier integration (Bennett & Klug, 2012). The less integrated C-suppliers used different modes, structures, and frequencies of transport, which were not linked and coordinated by the car manufacturer.

The analysis of the delay times of the milk-run transport network (see section 4.1.2) showed that it was important to evaluate the relationship between phase coherence and phase offset. Stability regions of specific delay time intervals were calculated, which guaranteed a high degree of synchronicity (see Figure 6). We transferred these results and investigated the effect of delay time on the most important nodes of a just-in-sequence transport network between a car manufacturer and a JIS supplier. To investigate the synchronization of JIS suppliers in more detail, we selected the main supplier for seat sets. The module assembly plant of the 1-tier supplier was located at a regional distance from the car assembly plant, where a full truck load (FTL) of 15 seat sets (including the driver’s seat, passenger seat, and back seat) was delivered every 15 min on average. The seat sets ordered by the OEM were delivered according to the sequence call-off.

Figure 9 depicts the interaction between the coupling constant, as an indicator of the organizational coupling (EDI, spare trucks, etc.), and the delay time and the transport period offset. Transport periods varied from 15 min by ± 50 s ($\Delta\omega_{RAS} = 0$ to $\Delta\omega_{RAS} = 1.5$). All the four examples shown clearly indicated the negative correlation between the phase coherence r_{RAS} with the delay time, the transport period offset, and the coupling strength. As shown earlier, the relationship between r_{RAS} and delay time was highly nonlinear and sensitive. We observed a phase transition from the near-perfect synchronization to the propagating spatial wave patterns when the delay time and the frequency detuning were increased. This type of three-dimensional synchronization wave represented critical areas where phase entrainment was suddenly lost. Another interesting aspect was the formation of the stability plateaus of phase-locked regions (areas marked in red), which guaranteed a high degree of process coherence only in a relatively small parameter range. The transport period offset showed a high sensitivity to synchronization, which clearly indicated that the strong couplings of a transport system did not automatically generate synchronized transport processes even when the transport information was transferred in real time.

Upon the linking of the synchronization of transport processes with productivity, the results supported the empirical evidence in the lean management context. This crucial relationship has been described by, among others, the Theory of Swift, Even Flow by Schmenner and Swink (1998); that is, the productivity of any process increases with an increase in the speed by which goods flow through the process (in our case, transport speed), and it decreases with an increase in the variability associated with the steps in the process (in our case, transport operations). In general, one can state

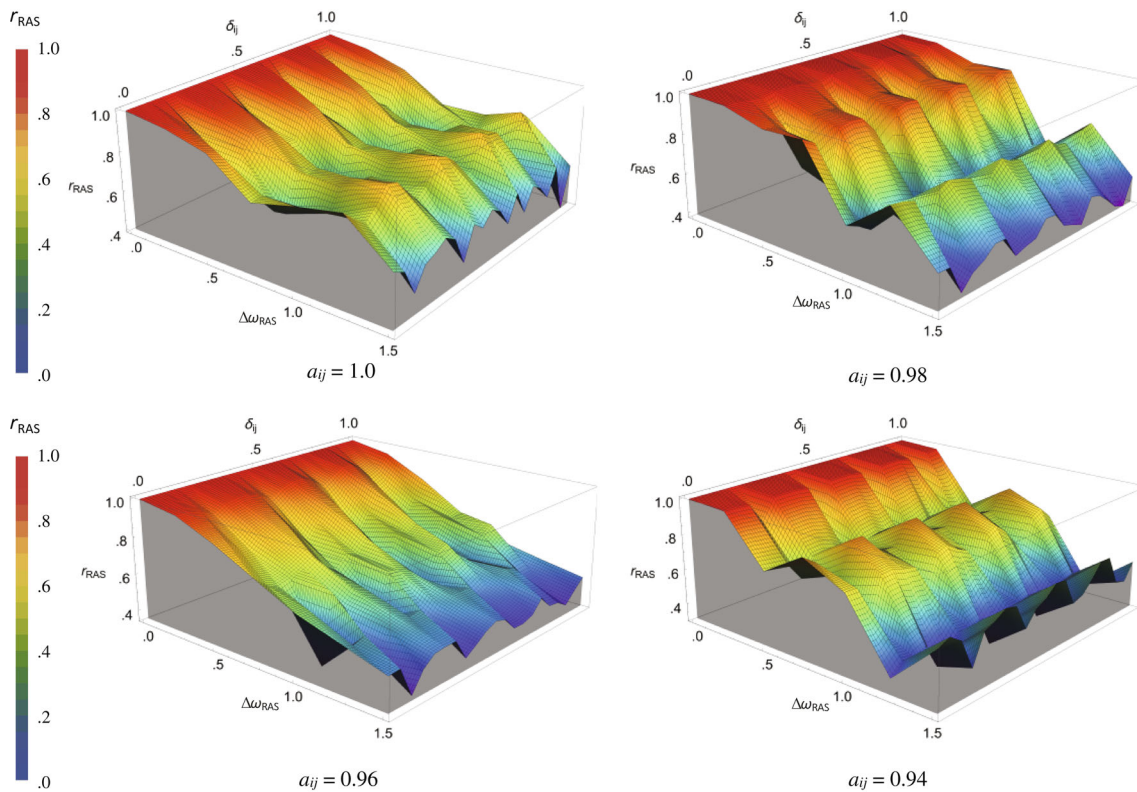


FIGURE 9 Comparison phase coherence r_{RAS} for different coupling constants a_{ij} with variations of delay time δ_{ij} [h] and transport period offset $\Delta\omega_{RAS}$ [h^{-1}]

that the period offset and the delay time act as a desynchronization force, while the coupling strength, as a strength of phase adjustment, determines the synchronization force. These three parameters define a three-dimensional space in which the phase-locking among transport processes can be determined. It is important to emphasize that phase locking is an intrinsic dynamical effect, which only provides the basis for transport control to adjust the transport frequencies and thus improve the overall transport synchronization. Thus far, all our investigations for the JIS transportation network were conducted under the assumptions of weakly interacting oscillators, where interactions led to phase adjustments without any strong perturbations induced by the transport management. Transportation systems are driven by outside influences, mainly influenced by disruptions causing delays. It is therefore necessary to react to the external disturbances of a transport system with implicit measures. Simulated parameter constellations as shown in Figure 9 of the JIS supply process can act as the quantitative basis for a dynamical continuous control of the JIS supply during its operation by manipulating the transport control signals. Figure 10 illustrates how a real-time control system of the seat supply process can be improved with by using an oscillatory model. An adaptive control mechanism to automatically cancel critical parameter constellations can be developed by readjusting the internal parameters of the JIS system. Based on the actual time delay (actual δ_{ij}) and the actual transport period offset $\Delta\omega_{RAS}$, a target value is calculated for the optimum delay time (target δ_{ij}). The main parameter to react to synchronization perturbations

is the transport pick-up time for the supplier and the transport order for the carrier. Control is achieved by a sporadic external interaction $\Delta\delta_{ij}$. By delaying or accelerating the transport periods, a detuned coupled supply process, which was slightly out of step, can be easily resynchronised without changing the amplitude (seat batch size). This task is performed by the truck supply control system of the car manufacturer, which calculates the necessary phase shift $\Delta\delta_{ij}$ within seconds to force the actual phase into the target phase. For each delivery cycle (every 15 min), a new truck handling schedule and time slot schedule for the pick-up and delivery times is calculated, adjusted, and transmitted to the supplier and the carrier.

5 | CONCLUSION

Improper synchronization can lead to transitions and instabilities, which cause very complex dynamics in transportation networks. The aim of this study was to introduce a new approach to better assess the synchronization of transport processes and to improve the knowledge of how synchronization is created and maintained in a transportation network. A network model that quantified transport relations based on oscillations that are generally difficult to analyze because the interaction functions of transport processes in a network can have many arbitrary Fourier harmonics was introduced. We showed that a phase representation in the form of a transport synchronization matrix

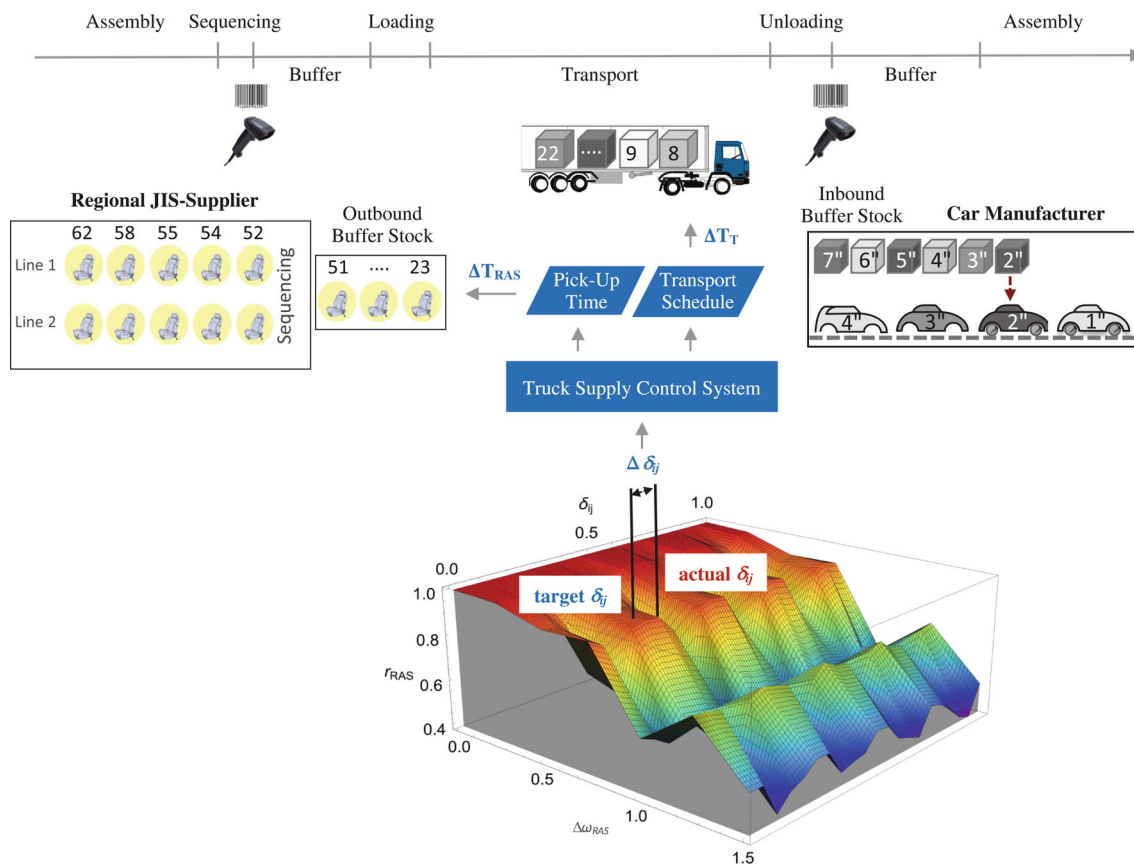


FIGURE 10 Adaptive mechanism for controlling just-in-sequence transports

(see Figures 4 and 7) was a compact visual representation that depicted different synchronization regimes throughout the transport network. Using the example of a milk-run in the automotive industry, we investigated how transport processes suddenly decoupled when the delivery frequency changed. This threshold value was used to define the stability criteria for the route planning of dynamic milk-runs. A further investigation of the milk-run stability showed how sensitively a ring topology reacted to delay times of transport information. Subsequently, a just-in-sequence transport network was investigated and examined more closely with respect to its stability against the changes in the delivery frequency and the time delays. Based on these results, an adaptive control mechanism was developed to re-synchronize a detuned supply process, by readjusting the internal parameters of a just-in-sequence transportation control system.

A future goal in the continuation of this work is the extension of the problem-specific application of the synchronization concept in the field of transport management. As Drexel (2012) stated: “The types of synchronization requirements that are present in a real-world application, an academic problem, or a mathematical model are always a matter of perspective and/or a modeling decision.” This also requires an evaluation of synchronization from a cost and performance perspective, which leads to the demand for new valuation

approaches. In general, better coordination of transport processes often requires investments such as in tracking and tracing systems. These costs have to be evaluated accordingly and compared with the services provided through improved process consistency. Maximum synchronization is not automatically the optimal synchronization and therefore requires additional cost and investment considerations. Finally, the question of how our results can be applied to other network topologies arises. Although ring and tree structures, as used in this study, are common network topologies, there are many other layouts (such as grid, hub-and-spoke, and small world networks) that are relevant to the context of transportation management (Zhang et al., 2015).

ACKNOWLEDGMENT

I would like to thank the DE, the AE, and the referees for their careful and constructive comments and suggestions that led to this improved version. Open Access funding enabled and organized by Projekt DEAL.

DATA AVAILABILITY STATEMENT

The data that support the findings of this study are available on request from the corresponding author. The data are not publicly available due to privacy or ethical restrictions.

ORCID

Florian Klug  <https://orcid.org/0000-0002-2826-2294>

REFERENCES

- Balachandran, V., & Perry, A. (1976). Transportation type problems with quantity discounts. *Naval Research Logistics Quarterly*, 23(2), 195–209.
- Baumol, W. J., & Vinod, H. D. (1970). An inventory theoretic model of freight transport demand. *Management Science*, 16(7), 413–421.
- Bavarez, E., & Newell, G. F. (1967). Traffic signal synchronization on a one-way street. *Transportation Science*, 1(2), 55–73.
- Bennett, D., & Klug, F. (2012). Logistics supplier integration in the automotive industry. *International Journal of Operations and Production Management*, 32(11), 1281–1305.
- Blumenfeld, D. E., Burns, L. D., & Daganzo, C. F. (1991). Synchronizing production and transportation schedules. *Transportation Research Part B*, 25(1), 23–37.
- Chankov, S. M., Becker, T., & Windt, K. (2014). Towards definition of synchronization in logistics systems. *Procedia CIRP*, 17, 594–599.
- Chen, Q., Huang, K., & Ferguson, M. R. (2021). Capacity expansion strategies for electric vehicle charging networks: Model, algorithms, and case study. *Naval Research Logistics*, 69(3), 442–460.
- Donner, R. (2008). Multivariate analysis of spatially heterogeneous phase synchronisation in complex systems: Application to self-organised control of material flows in networks. *The European Physical Journal B*, 63(3), 349–361.
- Donner, R., Hofleitner, A., Höfener, J., Lämmer, S., & Helbing, D. (2007). Dynamic Stabilization and Control of Material Flows in Networks and its Relationship to Phase Synchronization. Proceedings of the 3rd International IEEE Scientific Conference on Physics and Control, Potsdam, Germany, September 3-7, 2007.
- Drexl, M. (2012). Synchronization in vehicle routing – A survey of VRPs with multiple synchronization constraints. *Transportation Science*, 46(3), 297–316.
- Dunbar, W. (2007). Distributed receding horizon control of dynamically coupled nonlinear systems. *IEEE Transactions on Automatic Control*, 52(7), 1249–1263.
- Evans, G. W. (1958). A transportation and production model. *Naval Research Logistics Quarterly*, 5(2), 137–154.
- Fessler, J. A., & Sutton, B. P. (2003). Nonuniform fast Fourier transforms using min-max interpolation. *IEEE Transactions on Signal Processing*, 51(2), 560–574.
- Gan, X., & Wang, J. (2013). The synchronization problem for a class of supply chain complex networks. *Journal of Computers*, 8(2), 267–271.
- Glover, F., Klingman, D., & Ross, G. T. (1974). Finding equivalent transportation formulations for constrained transportation problems. *Naval Research Logistics Quarterly*, 21(2), 247–253.
- Göksu, A., Kocamaz, U. E., & Uyaroglu, Y. (2015). Synchronization and control of chaos in supply chain management. *Computers & Industrial Engineering*, 86, 107–115.
- He, Q., Irnich, S., & Song, Y. (2019). Branch-and-cut-and-Price for the vehicle routing problem with time windows and convex node costs. *Transportation Science*, 53(5), 1409–1426.
- Helbing, D., Lämmer, S., Seidel, T., Šeba, P., & Platkowski, T. (2004). Physics, stability, and dynamics of supply networks. *Physical Review E*, 70(6), 66–116.
- Ibarra-Rojas, O. J., & Rios-Solis, Y. A. (2012). Synchronization of bus timetabling. *Transportation Research Part B*, 46(5), 599–614.
- Kang, L., Zhu, X., Sun, H., Puchinger, J., Ruthmair, M., & Hu, B. (2016). Modeling the first train timetabling problem with minimal missed trains and synchronization time differences in subway networks. *Transportation Research Part B*, 93, 17–36.
- Kelley, J. E. (1955). A dynamic transportation model. *Naval Research Logistics Quarterly*, 2(3), 175–180.
- Klug, F. (2017). Analysing the interaction of supply chain synchronisation and material flow stability. *International Journal of Logistics Research and Applications*, 20(2), 181–199.
- Klug, F. (2018). Logistikmanagement in der Automobilindustrie – Grundlagen der Logistik im Automobilbau. Springer Verlag.
- Klug, F. (2022). Modelling oscillations in the supply chain: The case of a just-in-sequence supply process from the automotive industry. *Journal of Business Economics*, 92(1), 85–113.
- Kuramoto, Y., & Arakai, H. (1984). Chemical oscillations, waves, and turbulence. Springer.
- Lämmer, S., Kori, H., Peters, K., & Helbing, D. (2006). Decentralised control of material or traffic flows in networks using phase-synchronisation. *Physica A*, 363(1), 39–47.
- Mardia, K. (1972). Statistics of directional data. Academic Press.
- Rosenblum, M. G., Pikovsky, A. S., & Kurths, J. (1997). From phase to lag synchronization in coupled chaotic oscillators. *Physical Review Letters*, 22(78), 4193–4196.
- Schmenner, R. W., & Swink, M. L. (1998). On theory in operations management. *Journal of Operations Management*, 17(1), 97–113.
- Sipahi, R., Lämmer, S., Helbing, D., & Niculescu, S.-I. (2009). On stability problems of supply networks constrained with transport delay. *Journal of Dynamic Systems, Measurement and Control*, 131(2), 021005.
- Strogatz, S. (2000). From Kuramoto to Crawford: Exploring the onset of synchronization in populations of coupled oscillators. *Physica D*, 143(1–4), 1–20.
- Tawfik, C., & Limbourg, S. (2019). A Bilevel model for network design and pricing based on a level-of-service assessment. *Transportation Science*, 53(6), 1609–1626.
- Tilk, C., Bianchessi, N., Drexl, M., Irnich, S., & Meisel, F. (2018). Branch-and-Price-and-cut for the active-passive vehicle-routing problem. *Transportation Science*, 52(2), 300–319.
- Vaario, J., & Ueda, K. (1998). An emergent modelling method for dynamic scheduling. *Journal of Intelligent Manufacturing*, 9(2), 129–140.
- Wong, R., Yuen, T., Fung, K. W., & Leung, J. (2008). Optimizing timetable synchronization for rail mass transit. *Transportation Science*, 42(1), 57–69.
- Xiao, F., Yang, H., & Ye, H. (2016). Physics of day-to-day network flow dynamics. *Transportation Research Part B*, 86, 86–103.
- Zhang, X., Miller-Hooks, E., & Denny, K. (2015). Assessing the role of network topology in transportation network resilience. *Journal of Transport Geography*, 46, 35–45.

How to cite this article: Klug, F. (2023). Synchronization and stability in automotive transportation networks. *Naval Research Logistics (NRL)*, 70(2), 165–183. <https://doi.org/10.1002/nav.22089>

APPENDIX A

A discrete Fourier transform was used to empirically determine the oscillator frequencies of the individual transport processes (see Section 3.1). The signal used was a real-time scanning process performed when unloading the containers from the truck. Figure A1 shows an example of a periodic signal section of a just-in-sequence module delivery (see Section 4.2.1). The basic problem that arose upon the use of real discrete transport data was their non-equidistant sampling. By using a linear interpolation technique, the non-equidistant problem could be transformed into an equidistant (uniform) problem by resampling, which could then be analyzed using a uniform discrete Fourier transform (Fessler & Sutton, 2003).

A finite number N of samples of the signal $f[n]$ (scan signal) taken at regular intervals (after resampling) can be transformed into a function $F[k]$ of the temporal frequency, to be defined only at regular points of the frequency domain according to:

$$F[k] = \sum_{n=0}^{N-1} f[n] e^{-i\omega_n t_n} \quad k, n \in \{0, \dots, N-1\}. \quad (A1)$$

Considering that ω_n can assume only discrete values $k(2\pi/T)$ and $f[n]$ can assume only discrete values at times $t_n = n(T/N)$, it is possible to rewrite (A1) as:

$$F[k] = \sum_{n=0}^{N-1} f[n] e^{-i\left(k\frac{2\pi}{T}\right)\left(n\frac{T}{N}\right)} = \sum_{n=0}^{N-1} f[n] e^{-i\frac{2\pi}{N} kn}. \quad (A2)$$



FIGURE A1 Time series of an unloading signal section for a JIS delivery

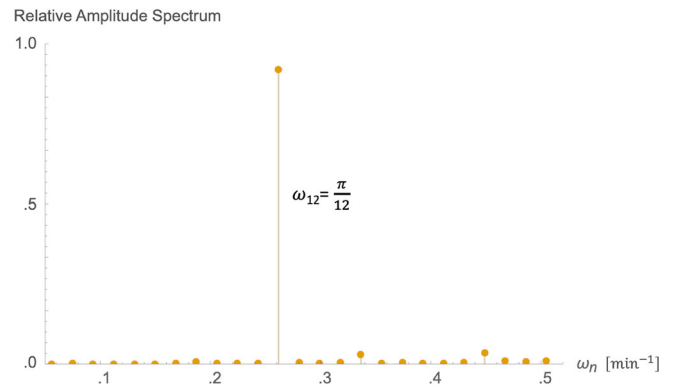


FIGURE A2 Relative amplitude spectrum JIS transport

By applying the discrete Fourier transform, the original time signal $f[n]$ was transformed into the frequency space. Figure A2 shows the analyzed frequency spectrum for the time series from Figure A1. The main transport frequency (fundamental frequency) is calculated with $\omega_n = .26 \text{ min}^{-1}$ with a relative amplitude share of 93%. These empirically determined main transport frequencies were used for the model parameterization. Due to the minute-precise acquisition of the transport data (see Section 3.1), the sampling (angular) frequency is calculated with $\omega_S = 2\pi \text{ min}^{-1}$. The smallest determined delivery interval of 19 min (JIS supplier) corresponds to a delivery frequency of $\omega_N = .33 \text{ min}^{-1}$ is thus less than half of the sampling frequency, so that the Nyquist theorem is always fulfilled.